Nature of Point Defects on SiO_2/Mo(112) Thin Films and Their Interaction with Au Atoms

Umberto Martinez, Livia Giordano, and Gianfranco Pacchioni*

Dipartimento di Scienza dei Materiali, Università di Milano-Bicocca, Via R. Cozzi, 53-20125, Milano, Italy

Received: June 13, 2006; In Final Form: July 3, 2006

We have studied by means of periodic DFT calculations the structure and properties of point defects at the surface of ultrathin silica films epitaxially grown on Mo(112) and their interaction with adsorbed Au atoms. For comparison, the same defects have been generated on an unsupported silica film with the same structure. Four defects have been considered: nonbridging oxygen (NBO, ≡Si—O•), Si dangling bond (E′ center, ≡Si•), oxygen vacancy (V_O, ≡Si—Si≡), and peroxo group (≡Si—O—O—Si≡), but only the NBO and the V_O centers are likely to form on the SiO_2/Mo(112) films under normal experimental conditions. The ≡Si—O• center captures one electron from Mo forming a silanolate group, ≡Si—O⁻, sign of a direct interaction with the metal substrate. Apart from the peroxo group, which is unreactive, the other defects bind strongly the Au atom forming stable surface complexes, but their behavior may differ from that of the same centers generated on an unsupported silica film. This is true in particular for the two most likely defects considered, the nonbridging oxygen, ≡Si—O•, and the oxygen vacancy, ≡Si—Si≡.

1. Introduction

The structure and properties of metal nanoclusters supported on well-defined oxide surfaces or thin films is a topic of interest in surface science, cluster chemistry, material science, and nanotechnology.[1−3] Spectacular advances have been reached in the preparation of metal nanoclusters deposited on various supports and also as a result of the possibility of growing and characterizing at an atomistic level thin oxide films using photoelectron spectroscopies and atomic probes such as scanning tunneling microscopy (STM) or atomic force microscopy (AFM).[4−9] A substrate of great importance in catalytic applications is silicon dioxide. Deposition of transition metal clusters and particles on this oxide has been studied for catalytic applications.[10,11] These studies are dealing with the surface of amorphous silica, α-SiO_2, due to the difficulties in growing and preparing well-defined crystalline surfaces of this material. Only recently has the synthesis of a new crystalline phase of SiO_2 in the form of a thin film been reported by the group of Freund et al.[12−14] The substrate used is Mo(112), and the procedure consists of repeated cycles of Si deposition and subsequent oxidation, followed by a final annealing at $T > 1100$ K. Low-energy electron diffraction (LEED) pictures show a hexagonal, crystalline SiO_2 overlayer with c(2 × 2) periodicity. Antiphase domain boundaries split the silica epilayer into an array of silica crystal grains. The preparation procedure has been reproduced in the group of Goodman et al.[15−22] The structure of the films has been subject to an intense debate. STM images show that the films are flat, homogeneous,[15] and defect-free.[16,23] The structural aspects have been investigated in a series of papers,[16,23−25] and the issue has been resolved recently with the help of theoretical calculations.[23,25,26] The film consists of a single layer of SiO_4 tetrahedra which share three oxygen atoms forming three Si—O—Si bridges with the forth oxygen directly bound to the Mo substrate.[23,26] This corresponds to a hexagonal two-dimensional film covering the entire surface with a thickness of only 3−4 Å. Recently, it has been found that the same surface can be prepared under oxygen-rich conditions, leading to a new phase where a layer of oxygen atoms is adsorbed on the Mo surface, below the silica layer.[27] The existence of this different phase has been found on the basis of shifts in the XPS spectra of the O 1s core levels and in the phonon spectra of the film. No other structural difference exists between the "oxygen-poor" phase and this new "oxygen-rich" phase.[27] In this study, we are dealing with the oxygen-poor structure.

The elucidation of the structure of the SiO_2/Mo(112) films opens up the possibility of theoretically modeling the deposition of metal atoms and clusters. The group of Goodman et al. have been particularly active in preparing small Pd and Au particles on this support and in studying their catalytic properties.[17,21] Formation of Pd clusters has been studied also by Lu et al.[28] In a recent study, we have considered the properties of supported Pd and Au atoms on SiO_2/Mo(112).[29] The calculations, performed at the DFT-GGA level with a periodic supercell approach, have been done both for pure silica surfaces and for silica films supported on Mo(112), thus taking into account the effects of the metal−oxide interface. On the regular, defect-free silica films, the adsorption of metal atoms is very weak, and only in the presence of doped films, e.g., by Ti atoms, is it possible to bind sufficiently strongly the metal atoms arriving from the gas phase. Due to the small diffusion barriers, metal atoms like Au diffuse almost freely on the surface at room temperature and even below.[29]

Defects on crystalline silica films have been studied using UV photoelectron spectroscopy and metastable impact electron spectroscopy techniques.[16] Generally, three major defects are expected to be present in the silica films: extended defects (steps and kinks), line defects (antiphase domain boundaries), and point defects (oxygen vacancies).[30] Defect-poor and defect-rich silica films have been prepared by changing the preparation method and used to study the nucleation of Pd particles on the two surfaces. On high-defect SiO_2, Pd clusters with diameter of 2−3 nm are distributed relatively homogeneously. This is in contrast to the low-defect surface, where the Pd cluster density dramatically decreases, and the cluster diameters are on the order of

* Corresponding author. E-mail address: gianfranco.pacchioni@unimib.it.

10.1021/jp063681e CCC: $33.50 © 2006 American Chemical Society
Published on Web 08/04/2006

3−6 nm.[30] To investigate the influence of defects on the nucleation of Au, silica films with a high density of defects have been prepared using an annealing temperature of 1100 K.[31] While on low-defect films the Au clusters nucleate along the line defects, on the high-defect film the clusters nucleate primarily on the terrace sites. The results also show that the cluster density correlates with the number of point defects.[31] In this as well as in other studies from Goodman's group, it was suggested that the most probable defects are oxygen vacancies, since silanol groups are unlikely given the high annealing temperature.[31,17,22] However, nonbridging oxygens could form under these conditions.

This theoretical study represents a first contribution to understanding the nature and the properties of specific point defects present on SiO_2/Mo(112) films. We have considered a few defects which are known to exist in various concentrations on the surface of chemically or mechanically activated silica.[32,33] These are the nonbridging oxygen, NBO or ≡Si—O•, the Si dangling bond, E′ center or ≡Si•, the oxygen vacancy, V_O or ≡Si—Si≡, and the peroxo group, ≡Si—O—O—Si≡. The nature of these defects in the bulk of silica has been the subject of several studies,[34] while fewer efforts have been devoted to the characterization of the surface counterparts. Here, we are interested in the specific structural and energetic features of these centers formed on crystalline SiO_2/Mo(112) films. Given the specific nature of these films and the presence of a metal support, it is not clear that the structure of the defects will be the same as in bulk silica. Thus, for comparison, we have considered an unsupported silica film with the structure of SiO_2/Mo(112). This pure silica film is obtained by combining two hexagonal SiO layers, and the resulting surface corresponds to a wall of the MCM-41 zeolite.[35] The surface is completely hydrophobic and hydroxyl-free.

2. Computational Details

We performed gradient-corrected density functional theory (DFT) calculations using the PW91 exchange-correlation functional.[36] The method is implemented in the VASP program,[37,38] which uses a plane wave basis set (kinetic energy cutoff at 400 eV). The electron−ion interactions are described by the projector-augmented wave method (PAW) developed by Blöchl.[39] This is basically an all-electron frozen-core method combining the accuracy of all-electron methods with the computational simplicity of the pseudopotential approach. The atoms within the supercell are relaxed until the atomic forces are less than 0.01 eV/Å. The pure silica surface has been modeled by a Si_2O_5 bilayer structure.[26]

Various binding modes exist for the interface oxygen atom in direct contact with the Mo substrate in SiO_2/Mo(112) (see ref 23). The structure where one O atom of the SiO_4 group is in a bridge position over two Mo atoms is the most stable one and has been used in this work. The Mo(112) substrate has been modeled by seven Mo layers which reproduce well the band structure of bulk Mo.[24] During geometry optimization, all Si and O atoms and all Mo atoms in the four surface nearest-layers were relaxed, while the atom positions for the remaining three Mo layers were frozen at bulk positions. The c(2 × 2) pattern is respected for one monolayer films whose supercell stoichiometry is $Mo_{14}Si_2O_5$ (hexagonal structure). When a Au atom is adsorbed or a point defect is created, the cell size changes to represent a low concentration of adsorbates or dopants. In particular, we used a (4 × 2) cell with one metal atom or one point defect every eight Si atoms; the cell becomes $Mo_{56}Si_8O_{20}$.

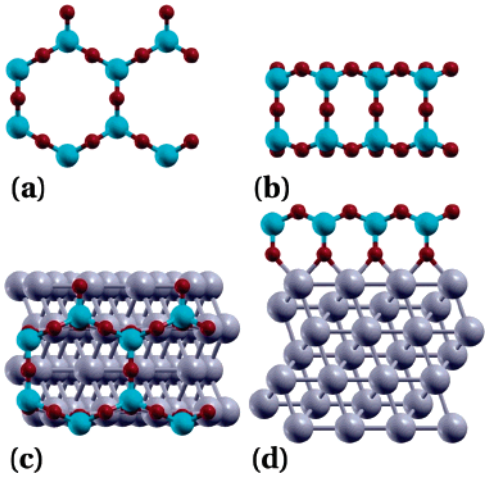

Figure 1. (a) Top view and (b) side view of the unsupported SiO_2 bilayer with the structure of MCM-41; (c) top view and (d) side view of a SiO_2/Mo(112) film.

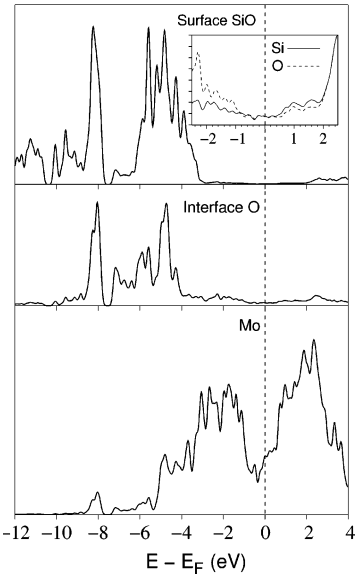

Figure 2. Projected DOS of a nondefective SiO_2/Mo(112) film.

The calculations have been done in a 2 × 2 × 1 grid of *k*-points. The surface slabs are separated by a vacuum slab of 10 Å.

3. Point Defects on SiO_2 and SiO_2/Mo(112) Films

We first discuss briefly the geometric and electronic structure of a SiO_2 bilayer and of the nondefective SiO_2/Mo(112) film (for details, see refs 23−26). Figure 1a,b shows a top view and a side view, respectively, of a wall of the MCM-41 zeolite structure. At the PW91 level, this low-dimensional material exhibits a gap of 5.4 eV, i.e., substantially reduced with respect to that of pure silica, ∼9 eV, partly due to the known limitations of DFT in reproducing the energy gap of insulators and partly because of the low dimensionality of the system and of its extended surface.

The silica film can be adapted to the Mo(112) substrate by forming direct bonds of the Mo atoms with the SiO bonds of the silica film, Figure 1c,d. The density of states (DOS) curves of the nondefective SiO_2/Mo(112) film, Figure 2, provide some information about the electronic structure of the system. The top of the O 2p band is about 3 eV below the Fermi level (E_F); the O atoms at the interface between Mo and the silica film contribute significantly to the DOS at E_F because of their strong mixing with the Mo 4d states. In addition, the top SiO layer,

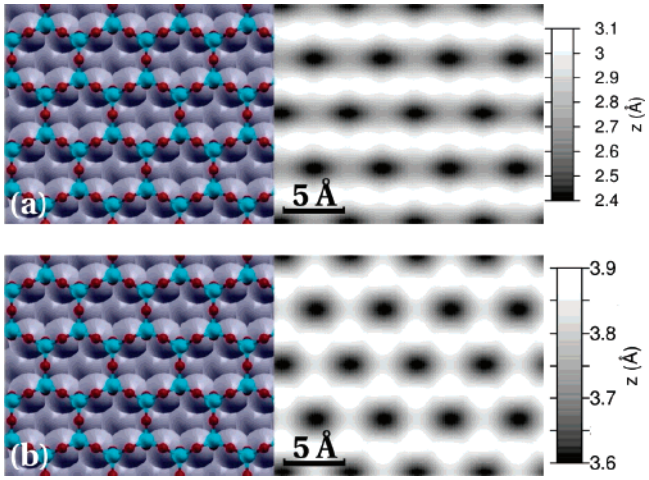

Figure 3. Simulated STM images of the nondefective SiO_2/Mo(112) film at (a) $V = 0.65$ V and (b) $V = 1.20$ V.

however, shows a nonzero contribution to the DOS at E_F. This is better shown in the inset of Figure 2 where only the region around E_F is represented. In this respect, the electronic structure of the supported silica film differs from that of the unsupported film for which no states are present in the gap (not shown). Of course, this is true for a nondefective structure. In the following, we consider the geometric structure of some point defects and how they perturb the electronic structure of the system.

The presence of metal-induced gap states, Figure 2, allows one to image with STM the structure of the film. Accurate STM images of SiO_2/Mo(112) have been reported together with their simulation[23,25] from the self-consistent charge density employing the Tersoff−Hamann approach.[40] Using the same approach, we have determined the simulated images of some defects present on the surface of the film (in particular, we considered the two most probable defects, the NBO center and the oxygen vacancy; see below). These can be compared with the image of the nondefective film, Figure 3 (the images are simulated at a positive bias $V = 0.65$ eV and $V = 1.20$ eV, as in the experiment).

3.1. Nonbridging Oxygen (NBO): SiO_2 Film. The NBO center is a classical defect in SiO_2. It consists of an unpaired electron localized in a nonbonding 2p orbital of a terminal oxygen atom. The EPR and optical absorption spectra of NBO in bulk silica are known and have been investigated both experimentally and theoretically.[34] In the unsupported silica bilayer, the NBO center has been generated by breaking a Si−O−Si bond connecting the two SiO layers (Figure 1b). This leads to the formation of two radical structures, ≡Si−O• (NBO) and ≡Si•, the E′ center, corresponding to a triplet state in the calculation. The formation energy of this pair of defects is 5.96 eV (Table 1), which corresponds to the strength of the Si−O bond. The formation of two radical centers is not the only possible solution. In fact, another possibility is that the two electrons are paired in a single orbital giving rise to a charge transfer (CT) structure: the unpaired electron of the ≡Si• center is transferred to the ≡Si−O• defect, with formation of two charged species, $\equiv Si^+$ and $\equiv Si-O^-$, respectively (see the inset of Figure 4b). The opposite process, formation of $\equiv Si^-$ and $\equiv Si-O^+$, is highly unfavorable, as ≡Si−O• has a much higher electron affinity and ionization potential than ≡Si•. The calculations show that the closed-shell CT solution is 0.53 eV more stable than the biradical structure. The CT occurs because the cost to ionize the ≡Si• defect is partially compensated by the gain of adding one electron to ≡Si−O•; the fact that the two centers are separated by a small distance provides an additional electrostatic stabilization. Still, the formation energy remains quite high, 5.43 eV (Table 1).

Not surprisingly, the two structures, biradical and CT, have quite different geometries. In particular, the $\equiv Si-O^-$ center has a short Si−O bond, 1.55 Å, compared to the neutral ≡Si−O• defect, 1.65 Å. A cluster model calculation of the isolated $\equiv Si-O^-$ and ≡Si−O• groups formed on edingtonite[41] gives essentially the same distances obtained in the periodic calculation for the two structures, thus providing additional evidence of the formation of a charged species. The other clear sign that a CT has occurred is in the structure of the ≡Si• center. In the neutral form, this is pyramidal, while it becomes nearly planar in the charged version, $\equiv Si^+$ (Figure 4b), consistent with the sp^3 and sp^2 nature, respectively, of the hybrid orbitals formed by the central silicon atom.

The two defects, ≡Si−O• and $\equiv Si-O^-$, induce important changes in the DOS of the unsupported silica film (Figure 4a,b). Neutral NBO is characterized by a singly occupied 2p level of the terminal oxygen just above the top of the valence band (Figure 4a). The NBO^- defect introduces two new states in the band gap at about 1.0 and 2.5 eV above the top of the valence band (Figure 4b). The presence of an extra electron in the 2p levels of the singly coordinated O atom shifts all its valence levels to higher energies. These donor states are particularly reactive, as they can interact and transfer charge to an adsorbed species.

3.2. Nonbridging Oxygen (NBO): SiO_2/Mo(112). On the supported film, the generation of an NBO defect implies the rupture of a Si−O···Mo interface bond, with inversion of the ≡Si−O• fragment toward the vacuum to avoid the recombination. The first question to answer is weather this defect center is charged or not, since the formation of $\equiv Si-O^-$ can occur at the expense of the Mo metal. In particular, if the Fermi level of Mo lies above the empty states of the neutral ≡Si−O• fragment, a CT can occur spontaneously. This is indeed the case, and the proof is the short Si−O distance, 1.55 Å, which coincides with that calculated for $\equiv Si-O^-$ in a cluster calculation.[41] Furthermore, the ground-state solution for the SiO_2/Mo(112) film where an NBO center has been created is non-spin-polarized, since the electron is removed from the metal valence band and the resulting hole is completely delocalized. It is interesting to note that the formation energy of this defect, 3.43 eV (Table 1), is about 2 eV lower than in the unsupported silica film. The electronic structure (Figure 5a) closely resembles that of the

TABLE 1: Formation Energies, ΔE in eV, of Various Defects Generated on the Unsupported SiO_2 Film and on SiO_2/Mo(112)[a]

	ΔE(NBO)	ΔE(E′)	$\Delta E(V_O)$[b]	ΔE(peroxo)[b]
SiO_2	5.43 (≡Si−O⁻; $\equiv Si^+$)	5.96 (≡Si•; ≡Si−O•)	8.85 (≡Si−Si≡)	−1.27 (≡Si−O−O−Si≡)
SiO_2/Mo(112)	3.43 (≡Si−O⁻)	2.95 (≡Si•, Mo═O)	8.74, 8.94 (2.60)[c] (≡Si−Si≡)	−1.37 (≡Si−O−O−Si≡)

[a] The electronic nature of the defect is specified in parentheses. [b] The values are computed with respect to a free oxygen atom. [c] Computed with respect to an oxygen atom adsorbed on Mo.

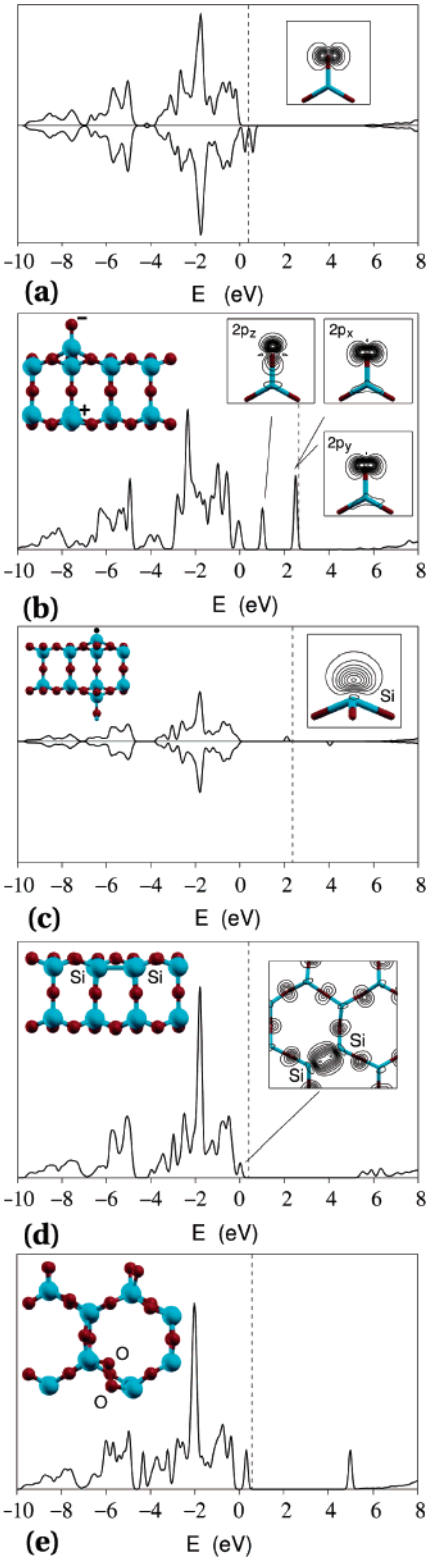

Figure 4. DOS of the unsupported SiO_2 film: (a) ≡Si—O• defect (minority and majority spin); the inset shows the spin density plot of the singly occupied O 2p state. (b) ≡Si—O^- charged center; inset 1 shows the structure of the ≡Si—O^-/≡Si^+ pair of defects (see text); inset 2 shows the charge density plots of the three O 2p orbitals of the terminal oxygen atom. (c) ≡Si• defect; inset 1 shows the geometric structure of the defect obtained by saturating with an H atom the ≡Si—O• center resulting from the breaking of the ≡Si—O—Si≡ bond; inset 2 shows the spin density of the center. (d) ≡Si—Si≡ defect; inset 1 shows a side view of the geometric structure of the defect; inset 2 shows the charge density of the doubly occupied level corresponding to the ≡Si—Si≡ bond. (e) ≡Si—O—O—Si≡ defect; the inset shows a top view of the geometric structure of the defect.

unsupported film with a ≡Si—O^- defect (Figure 4b), with two filled levels well above the O 2p valence band.

The simulated STM images for the ≡Si—O^- center are shown in Figure 6a. At positive bias, one is tunneling through the empty states of the defect, and the image appears as a bright spot protruding from the surface. This is even more pronounced if one is tunneling at negative bias, through the filled states of the defect, which appears as a large ring structure due to the O $2p_x$ and $2p_y$ states of dimensions comparable to those of a silica ring.

3.3. Silicon Dangling Bond (E′): SiO_2 Film. We have seen above that the creation of two radical centers, ≡Si—O• (NBO) and ≡Si• (E′), by breaking a Si—O—Si bond in the unsupported SiO_2 bilayer is unfavorable and leads to a pair of charged defects. Therefore, to study the properties of the isolated ≡Si• E′ center, we have saturated the ≡Si—O• defect with a H atom, forming a hydroxyl group, ≡Si—OH. In this way, the remaining unpaired electron is localized on the three-coordinated Si atom, as shown by the spin density plot (see inset of Figure 4c). Since the breaking of the Si—O—Si bond costs 5.96 eV (Table 1), this defect is energetically very unfavorable. If present, it induces a singly occupied state in the middle of the silica band gap, more than 2 eV above the top of the valence band (Figure 4c).

3.4. Silicon Dangling Bond (E′): SiO_2/Mo(112). The formation of the E′ center on the SiO_2/Mo(112) film implies the rupture of a Si····O—Mo bond. The process costs 2.95 eV (Table 1), i.e., much less than the energy required to break the Si—O bond in pure silica. The reason is that here the oxygen atom can bind very strongly to the Mo substrate forming a nearly double bond, Mo═O, partially compensating for the cost of the rupture of the Si—O bond. The resulting structure where the Si atom is oriented toward the vacuum is a local minimum separated by a small barrier, 0.07 eV, from the deep minimum corresponding to the Si and O recombination and formation of the original Si—O—Mo interface bond. The defect has radical character, at variance with the NBO case, and does not trap electronic charge coming from the Mo metal, because the ≡Si• empty state lies above E_F(Mo) (Figure 5b; the defect that remains formally neutral). The unpaired electron is localized on the Si atom, and the corresponding singly occupied energy level is almost 3 eV above the O 2p band (Figure 5b). The fact that this structure is metastable and readily converts into the much more stable nondefective structure suggests that it is very unlikely that this kind of defect will form on SiO_2/Mo(112) films. For this reason, the simulated STM images of this center are not reported.

3.5. Oxygen Vacancy (V_O): SiO_2 Film. In the unsupported SiO_2 bilayer, there are two nonequivalent oxygen atoms: one is in the surface plane; the second one is connecting the two SiO layers (Figure 1), and an oxygen vacancy can be created in these two positions. For the purpose of this work, the vacancy formed on the top layer is more interesting, as it will be a potential site for surface reactivity. Furthermore, the equivalent of the interlayer vacancy does not exist on the SiO_2/Mo(112) film or at least has a different structure, since it brings in direct contact a Si atom with the Mo metal (Figure 1d). Therefore, we restrict the analysis to the V_O center created on the surface layer; see inset of Figure 4d. The removal of a surface oxygen results in two ≡Si• dangling bonds, which recombine to form a direct ≡Si—Si≡ bond. The distance between the two Si atoms is 2.57 Å (it is 3.07 Å before oxygen removal), showing a strong relaxation induced by the defect formation, in full analogy with bulk SiO_2 (where the Si—Si distance becomes about 2.4−2.5 Å).[34] The formation energy of the defect, computed with respect

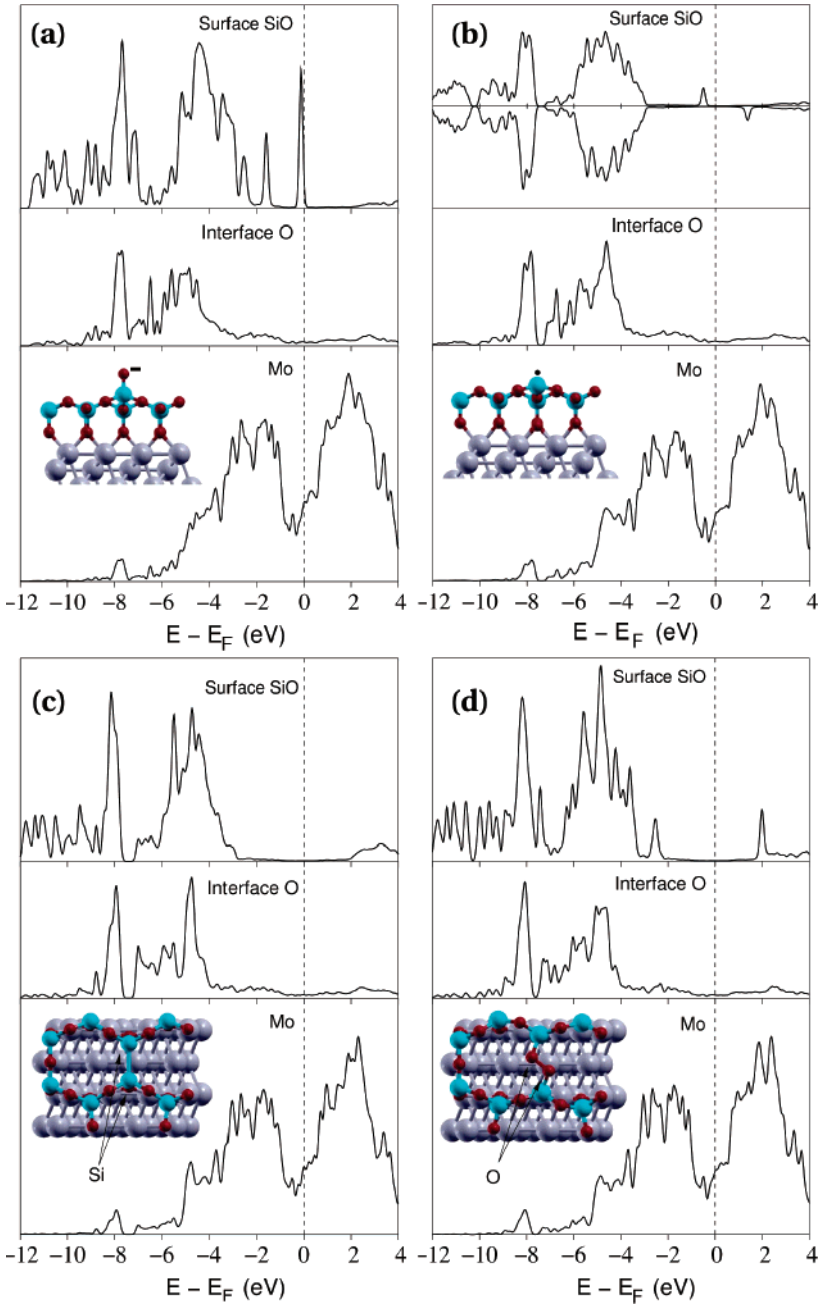

Figure 5. Projected DOS of the supported SiO_2/Mo(112) film: (a) ≡Si—O^- defect; the inset shows a side view of the geometric structure of the defect. (b) ≡Si• defect; the inset shows a side view of the geometric structure of the defect. (c) ≡Si—Si≡ defect; the inset shows a top view of the geometric structure of the defect. (d) ≡Si—O—O—Si≡ defect; the inset shows a top view of the geometric structure of the defect.

to a gas-phase oxygen atom, is very high, 8.85 eV, consistent with the fact that the Si—Si bond formed is much weaker than the two Si—O bonds broken. The localization of an electron pair between the two Si atoms is clearly shown by electron density maps, which also allows one to assign a peak in the DOS just above the top of the O 2p valence band to the V_O defect (Figure 4d). To this bonding state is associated an antibonding combination which is close to the silica conduction band.

3.6. Oxygen Vacancy (V_O): SiO_2/Mo(112). On the SiO_2/Mo(112) supported film there are two nonequivalent oxygen atoms in the top layer, corresponding to two different locations of the oxygen vacancy. Both have been considered, but their formation energies differ by 0.2 eV only, a small quantity compared to the cost of 8.74 eV required to create the defect (Table 1). Thus, there is virtually no difference in the cost of creating an oxygen vacancy in the pure silica bilayer or in the Mo supported silica film (Table 1). Also, the minimal Si—Si distance, 2.58 Å, is practically the same found on the unsupported film. Notice, however, that on SiO_2/Mo(112) an oxygen atom can be accommodated at the Mo surface, forming a strong bond of 6.1 eV. This reduces considerably the cost for creating the defect which, according to our calculations, becomes about 2.60 eV (Table 1). On this basis, it is quite possible that on films created under oxygen-poor conditions a given number of oxygen vacancies are present. This would not alter to whole stoichiometry of the film but only result in the "displacement" of an oxygen atom from the SiO top layer to the interface. The electronic structure of the film is only weakly perturbed by the formation of the defect. A state with Si—Si bonding character appears near the top of the O 2p valence band, while the rest of the occupied states are not affected (Figure 5c). The simulated STM images (Figure 6b) show an ellipsoidal spot due to the bonding and antibonding states of the defect.

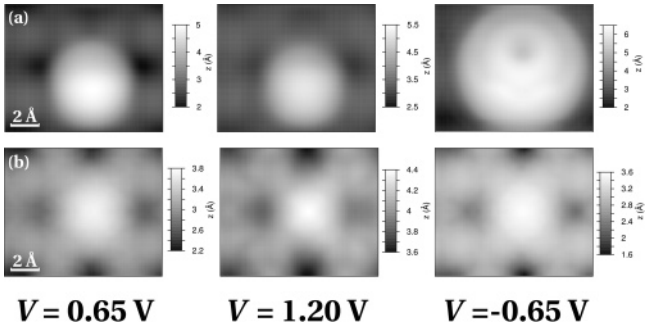

Figure 6. Simulated STM images of (a) ≡Si—O⁻ center formed on SiO_2/Mo(112) and (b) a ≡Si—Si≡ center formed on SiO_2/Mo(112). The images are simulated at $V = 0.65$ V, $V = 1.20$ V, and $V = -0.65$ V.

3.7. Peroxo Group: SiO_2 Film and SiO_2/Mo(112). The last defect considered is a peroxo group formed by addition of an oxygen atom the nondefective silica layer. This is the only defect whose formation energy, computed with respect to a free oxygen atom, is negative, −1.27 eV (exothermic reaction; Table 1). However, since the energy required to dissociate the O_2 molecule is 5.2 eV (experimental value), the formation of a peroxo group is thermodynamically unfavorable even in excess oxygen conditions. The structure of the resulting defect is that of a classical peroxo group in silicon dioxide, ≡Si—O—O—Si≡, with an O—O distance, 1.49 Å, typical of this kind of linkage. The creation of this defect results in two new levels, a filled state just above the top of the O 2p valence band and an empty state below the conduction band. The states are associated to π-type bonding and antibonding orbitals involving the two oxygen atoms.

The structure of the peroxo defect on the SiO_2/Mo(112) film is virtually indistinguishable from that of the unsupported silica bilayer. The formation energy, −1.37 eV (Table 1), is only slightly higher, and the geometrical parameters, r(O—O) = 1.48 Å and r(Si—O) = 1.67 Å, are the same as in the pure silica structure. In addition, the electronic structure is practically that found for the unsupported layer, with two impurity levels appearing in the structure (Figure 5d; for this reason, only the DOSs of the supported film are reported): a doubly occupied state is about 1 eV above the O 2p valence band, and an empty level is slightly below the SiO_2 conduction band but well above the Mo Fermi level. Therefore, no charge transfer is expected from the Mo metal to the empty states of this defect that remains neutral.

The computational results show that the additional oxygen atom preferes to bind at the interface with the Mo atom rather than be included in the silica lattice. This means that the peroxo group, which can be formed in conditions of excess oxygen, is rather unlikely to form on the ultrathin films, since this defect is unstable with respect to the displacement of the extra oxygen and its diffusion at the interface. In fact, the recent results obtained in the Freund's group show that in oxygen-rich conditions a new phase is formed characterized by the presence of interface oxygen atoms.[27]

4. Au Atoms Interacting with Point Defects on SiO_2 and SiO_2/Mo(112) Films

The interaction of Au atoms with a nondefective unsupported or supported silica film is very weak, and the computed interaction energies are on the order of 0.1 eV.[29] Therefore, only specific point or extended defects, when present, can stabilize the metal atoms, prevent diffusion, and favor nucleation and growth of a nanoparticle. In the following, we will discuss the properties of Au atoms adsorbed on the four point defects described in the previous section.

4.1. Au atoms on NBO center: SiO_2 film. We have seen above that there are two variants of the NBO center, the neutral paramagnetic one, ≡Si—O•, and the charged diamagnetic one, ≡Si—O⁻. This latter can be generated in bulk silica by effect of irradiation, according to the the reaction ≡Si—O• + $h\nu$ → ≡Si—O⁻. Clearly, the two forms of the defect will interact in a different way with an adsorbed Au atom. The Au atom, $5d^{10}$-$6s^1$ ground state, can form a direct covalent bond with ≡Si—O• by coupling the 6s electron with the unpaired O 2p electron. In the case of ≡Si—O⁻, there is an extra electron which must be accommodated into a high-lying antibonding O—Au σ molecular orbital. On both SiO_2 and SiO_2/Mo(112) films, this could result in a charge transfer to the adsorbed Au atom, with formation of Au⁻ (this process would be favored by the high electron affinity of Au, 2.3 eV in both theory and experiment). However, the extra electron can also be trapped by another defect site of the SiO_2 bilayer (provided that this defect has low-lying empty levels), or on SiO_2/Mo(112), it can be transferred to the Mo conduction band. In these case, one is left with a ≡Si—O—Au neutral complex.

On the unsupported silica layer, these possibilities can be checked by adsorbing a Au atom on the two different structures, ≡Si—O⁻/≡Si⁺ or ≡Si—O•/≡Si• (see section 3.1). No matter which is the initial structure, the final configuration of the surface complex is the same and corresponds to a ≡Si—O—Au neutral bond. In fact, Au forms a strong bond with the terminal oxygen with r(Au—O) ≈ 2 Å, and a Si—O—Au bond angle of about 120° (Figure 7a). The Si—O distance, 1.62 Å, is considerably longer than in ≡Si—O⁻ (1.55 Å), showing that that the formation of the Au—O bond starting from the ≡Si—O⁻/≡Si⁺ CT structure leads to a redistribution of charge. In particular, the extra electron of the NBO⁻ center is transferred to ≡Si⁺, which transforms into the neutral E′ center, ≡Si•. Thus, adsorption of Au to NBO or NBO⁻ leads to the same final structure, with a binding energy of 1.92 eV (Table 2) computed with respect to the ≡Si⁺/≡Si—O⁻ ground state (see sction 3.1). The fact that one electron is transferred from ≡Si—O⁻ to the ≡Si⁺ defect upon Au adsorption is not a normal situation. It occurs because on our system there is a deep electron trap represented by the electron-deficient ≡Si⁺ defect. In general, the silanolate group, ≡Si—O⁻, will interact with Au and form a charged complex, ≡Si—O—Au⁻. Recent studies on the optical properties of Au atoms deposited on an amorphous silica surface have shown that silanolate groups have a key role in binding the Au atoms and clusters.[41,42] The adsorbed Au atom introduces a number of states above the top of the O 2p valence band (Figure 7a).

4.2. Au Atoms on NBO Center: SiO_2/Mo(112). We consider now the same interaction with an NBO center on the SiO_2/Mo(112) film. We have seen above that the center becomes negatively charged, ≡Si—O⁻. The adsorption energy of Au on this site is 1.72 eV (Table 2), 0.2 eV smaller than on the NBO⁻ site of unsupported film, but sufficiently strong to guarantee that Au atoms trapped at this defect will be stable up to high temperatures. The structural properties of the complex are similar to those found for the unsupported silica layer, with an O—Au bond length of 2.02 Å and a Si—O—Au angle of 118° (Figure 8a). The analysis of the DOS curves (Figure 8a), and the fact that the system is non-spin-polarized, indicate that what is formed is basically a neutral ≡Si—O—Au complex. The

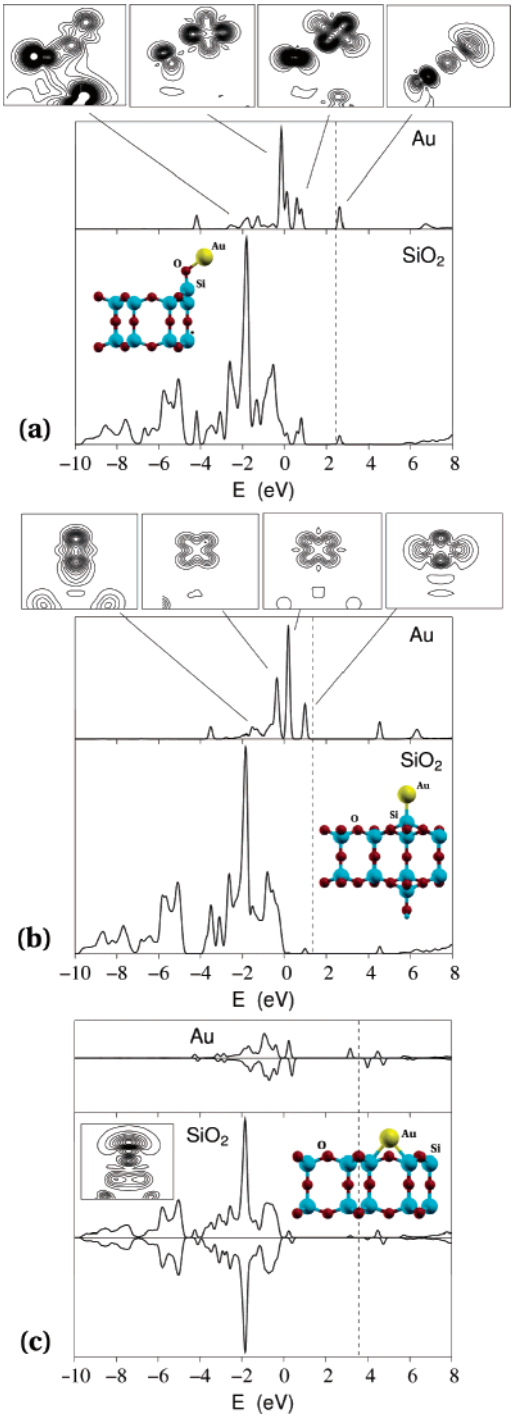

Figure 7. Projected DOS for a Au atom adsorbed on the unsupported SiO_2 film: (a) ≡S−O• defect; inset 1 shows a side view of the geometric structure of the ≡Si−O−Au complex; inset 2 shows the charge densities of the Au-derived states. (b) ≡Si• defect; inset 1 shows a side view of the geometric structure of the ≡Si−Au complex; inset 2 shows the charge densities of the Au-derived states. (c) ≡Si−Si≡ defect, minority and majority spin; inset 1 shows a side view of the geometric structure of the ≡Si−Au−Si≡ complex; inset 2 shows a spin density plot.

electron captured by the ≡Si−O• center from the Mo metal is transferred back to the metal substrate upon adsorption of gold.

4.3. Au Atoms on the E′ Center: SiO_2 Film. A gold atom binds to an E′ center of the silica surface with a strong bond, 3.52 eV (Table 2), and a Si−Au distance of 2.27 Å. The bonding is due to the coupling of the unpaired electron in the sp^3 hybrid orbital of the Si atom and the Au 6s electron with formation of a covalent bond. The Au−Si bond is perpendicular to the SiO plane of the unsupported silica film (Figure 7b). The Au 5d and 6s levels give rise to a series of occupied states at the top of the valence band or above it. The Si(sp^3)−Au(6s) σ-bonding combination is about 1 eV above the top of the valence band (Figure 7b); the corresponding antibonding combination is empty and close to the silica conduction band; the Au 5d orbitals are split by the interaction with the defect center (Figure 7b). Similar results have been reported recently for the interaction of a Au atom with an E′ center formed at the surface of Edingtonite.[41,42]

TABLE 2: Adsorption Energy (ΔE) and Selected Bond Distances for a Au Atom Interacting with Various Point Defects on an Unsupported SiO_2 Layer and a SiO_2/Mo(112) Film

	ΔE, eV	r(X−Au),[a] Å	r(Si−Si), Å
		SiO_2	
NBO	1.92	2.00	
E′	3.52	2.27	
V_O	1.18	2.39	2.99
		SiO_2/Mo(112)	
NBO	1.72	2.02	
E′	3.48	2.28	
V_O (1)[b]	0.94	2.55	2.56
V_O (2)[b]	1.80	2.29	4.49
V_O (3)[b]	2.87	2.37	3.75

[a] X = Si or O. [b] In the case of the supported film, data for the three minima found are reported (see text).

4.4. Au Atoms on the E′ Center: SiO_2/Mo(112). The bonding of Au to the E′ center of SiO_2/Mo(112) and SiO_2 films is similar. The binding energy is 3.48 eV (Table 2), and the Si−Au distance 2.28 Å, practically the same values obtained for the unsupported silica film. In this respect, the presence of the metal substrate does not affect the nature of the interaction with the E′ center, and the supported film behaves as a normal silica surface. Also, in this case, the Au adsorbate introduces filled levels above the O 2p valence band (Figure 8b). The strong bonding of the Si dangling bond to the Au atom suggests a high thermal stability of gold clusters anchored to the silica film by this kind of interaction.

4.5. Au Atoms on an O Vacancy: SiO_2 Films. Au binds to an oxygen vacancy on the unsupported SiO_2 layer by 1.18 eV (Table 2) and a Au−Si distance of 2.39 Å. The Si−Si distance increases to accommodate the Au atom, and in the final position becomes 2.99 Å, i.e., close to the original Si−Si distance in a normal Si−O−Si linkage (see inset in Figure 7c). In this respect, gold plays the role of the missing oxygen atom, taking its place in the bridge position and attracting charge from the Si neighbors because of its high electron affinity. Of course, Au is much bigger than O, so the atom remains well above the SiO surface plane (Figure 7c). The unpaired electron remains localized on the Au atom, as shown, for instance, by the spin density plots (see inset of Figure 7c).

4.6. Au Atoms on an O Vacancy: SiO_2/Mo(112). The adsorption of Au on an oxygen vacancy of the SiO_2/Mo(112) film presents a distinct character from the case of the unsupported silica layer. The effect of the substrate is important and results in a different potential energy profile. At least three minima are found as the Au atom approaches the surface defect (Table 2). The first minimum (1) is structurally and electronically similar (not identical) to that found on the unsupported film. The Au atom partially penetrates into the Si−Si bond and binds by 0.94 eV to the silica surface. In this structure, the two Si atoms have only slightly expanded their position, and their separation becomes 2.56 Å; the Si−Au bond length is 2.55 Å. A small barrier (not investigated in detail) separates this

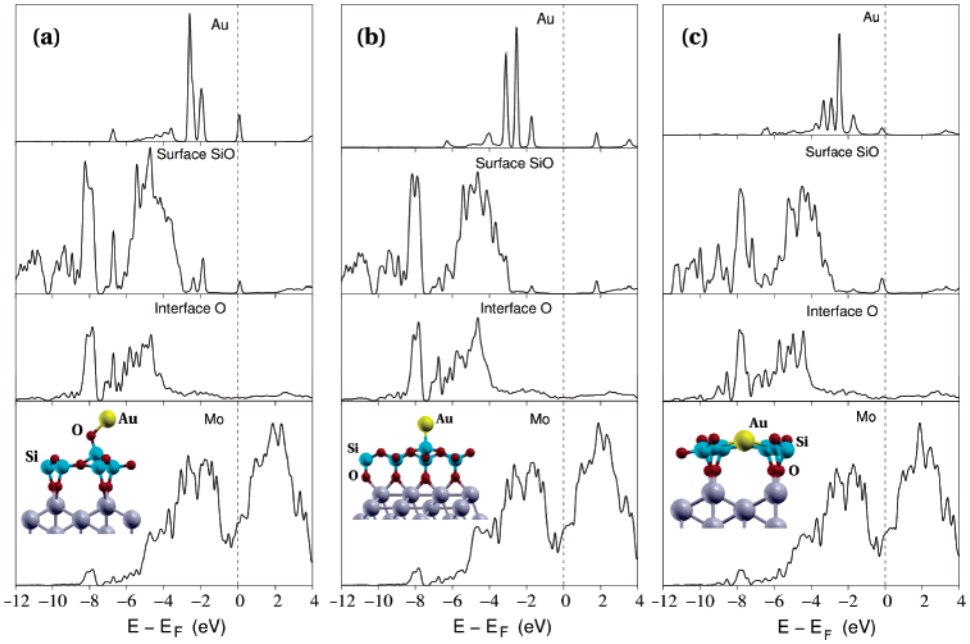

Figure 8. Projected DOS for a Au atom bound to the supported SiO_2/Mo(112) film: (a) ≡Si—O^- defect; the inset shows a side view of the geometric structure of the ≡Si—O—Au complex. (b) ≡$Si^•$ defect; the inset shows a side view of the geometric structure of the ≡Si—Au complex. (c) ≡Si—Si≡ defect; the inset shows a side view of the geometric structure of the ≡Si—Au—Si≡ complex, minimum (2), see text.

minimum from the next one where Au is bound by 1.80 eV. In this second minimum (2) (Table 2), the two Si atoms of the vacancy have moved apart to allow the penetration of Au into the SiO layer. The Si—Si distance becomes 4.49 Å, and the silica layer relaxes considerably to reduce the strain induced by the incorporation of Au (see inset of Figure 8c). Also, (2) is not the absolute minimum for the process. A barrier of about 0.15 eV separates the minimum (2) from the global minimum where the Au atom is incorporated at the SiO_2—Mo interface binding simultaneously to the two Si atoms of the vacancy and to the Mo substrate. The Au—Si distance becomes 2.37 Å, and the two Si atoms are separated by 3.75 Å. In this configuration, the energy gain is 2.87 eV (Table 2). Clearly, the interaction with Mo is the driving force that induces the penetration of Au into the silica film.

This result is the manifestation of a tendency observed already for other atoms such as Pd on the regular SiO_2/Mo(112) films.[29] The bonding of a metal atom at the SiO_2—Mo interface is much stronger than at the silica surface. Pd is small enough to penetrate with virtually no barrier into the hexagonal rings of the silica film to become incorporated between Mo and the SiO plane. This effect cannot occur with Au, which is too big with respect to the ring diameter.[29] The presence of an oxygen vacancy, however, opens a "door" into the perfect silica structure allowing diffusion below the oxide layer. This process implies relatively low barriers and in principle could occur already at low temperature, and in any case below room temperature (RT).

The analysis of the DOS curves for minimum (2) (Figure 8c) are similar to those of the global minimum and clearly show that the Au 6s state is completely filled and that the system is non-spin-polarized. This means that Au takes electrons from the Mo substrate and becomes negatively charged.

4.7. Au Atoms on a Peroxo Group: SiO_2 and SiO_2/Mo-(112) Films. A peroxo group on the silica surface is a nonreactive defect, at least toward Au. In fact, the calculations show that the interaction of this atom with the peroxo group is weak and similar to that found for the other sites of the nondefective surface. Only when the ≡Si—O···O—Si≡ bond is broken, with formation of two NBO centers, does the defect become an effective trapping site, but this implies overcoming the energy barrier needed to break the peroxo linkage.

The low reactivity also holds for the supported SiO_2/Mo-(112) film. In this case, we have analyzed what happens when the ≡Si—O···O—Si≡ bond is opened and a single Au atom is added. The Au atom binds to one end of the defect, forming a ≡Si—O—Au bond, while the rest of the structure undergoes a complex rearrangement. At the end of the process, one O atom is detached from the silica film and directly bound to Mo. This is another manifestation of the intrinsic instability of the peroxo group with respect to oxygen displacement to the interface. This complex rearrangement only occurs after the peroxo linkage has been broken, and it is therefore of little practical interest, since the barrier for the process is relatively high.

5. Conclusions

We have studied by means of periodic DFT calculations the structure and properties of point defects at the surface of ultrathin silica films epitaxially grown on Mo(112) and their interaction with adsorbed Au atoms. We restricted the analysis to films prepared in "oxygen-poor" conditions, consisting of a single SiO layer connected via interface oxygen atoms to the Mo substrate.[23,26] For comparison, the same defects have been generated on a pure silica film with the same structure. Four main defects have been considered: nonbridging oxygen (NBO, ≡Si—$O^•$), Si dangling bond (E′ center, ≡$Si^•$), oxygen vacancy (V_O, ≡Si—Si≡), and peroxo group (≡Si—O—O—Si≡). The results show that only the NBO and the V_O centers are likely to be formed on the SiO_2/Mo(112) films under normal experimental conditions. The E′ center in fact tends to recombine with an interface oxygen atom and form the undefective structure, while the peroxo group is unstable toward displacement of an oxygen atom to the interface. An interesting feature is that the ≡Si—$O^•$ center captures one electron from the Mo substrate, forming a silanolate group, ≡Si—O^-. All the defects introduce new states in the gap which can potentially be involved in the interaction with adsorbed metal atoms.

In the second part of the work, we have considered the interaction of a Au atom with the four point defects (the perfect

surface is completely unreactive toward these species).[29] Apart from the peroxo group, which is unreactive, the other defects strongly bind the Au atom, forming stable surface complexes. On ≡Si—O⁻, gold forms a neutral ≡Si—O—Au complex with a binding energy of 1.72 eV; the electron of the silanolate group is transferred back to the Mo metal upon Au adsorption. This is an example of interplay between the oxide film and the metal support that has no counterpart in the chemistry of the bare oxide surface. The ≡Si• center of SiO_2/Mo(112) forms a strongly bound ≡Si—Au complex (binding energy 3.48 eV) with characteristics very similar to those of the same bond formed on an unsupported silica film. The behavior of an oxygen vacancy, on the contrary, is completely different in the two cases. In the supported film, the vacancy acts as a "gate" where the Au atom can penetrate to bind more efficiently with the silica and the Mo substrate. In the minimum structure, Au is bound by 2.87 eV to the SiO_2/Mo(112) film. The structure of the complex is quite different from that found on the unsupported film where the metal atom remains above the silica surface and binds by 1.18 eV only.

In summary, point defects at the surface of SiO_2/Mo(112) act as strongly binding sites for adsorbed Au atoms, but their behavior may differ from that of the same centers generated on an unsupported silica film with the same structure. This is true in particular for the two most likely defects considered, the nonbridging oxygen, ≡Si—O•, which on the film transforms spontaneously into a silanolate group, ≡Si—O⁻, and the oxygen vacancy. So far, no evidence of the presence of point defects on the as-prepared SiO_2/Mo(112) films has been reported. In this respect, it is possible that the number of point defects has to be artificially increased in order to study their effect on adsorbed species.

Acknowledgment. This work is supported by the EU Project STREP GSOMEN and by the Italian Ministry of University and Research (Cofin 2005).

References and Notes

(1) Motoyama, Y.; Matsuzaki, H.; Murakami, H. *IEEE Trans. Electron Devices* **2001**, *48*, 1568.

(2) Weber, L. F. In *Flat-panel Displays and CRTs*; Tannas, L. E., Ed.; Van Nostrand Reinhold: Now York, 1985.

(3) Matulevich, Y. T.; Vink, T. J.; Zeijlmans van Emmichoven, P. A. *Phys. Rev. Lett.* **2002**, *89*, 167601.

(4) Freund, H.-J. *Surf. Sci.* **2002**, *500*, 271.

(5) Sanchez, A.; Abbet, S.; Heiz, U.; Schneider, W. D.; Ferrari, A. M.; Pacchioni, G.; Rösch, N. *J. Am. Chem. Soc.* **2000**, *122*, 3453.

(6) Sanchez, A.; Abbet, S.; Heiz, U.; Schneider, W. D.; Häkkinen, H.; Barnett, R. N.; Landmann, U. *J. Phys. Chem. A* **1999**, *103*, 9573.

(7) Bäumer, M.; Freund H.-J. *Prog. Surf. Sci.* **1999**, *61*, 127.

(8) Haas, G.; Menck, A.; Brune, H.; Barth, J. V.; Venables, J. A.; Kern, K. *Phys. Rev. B* **2000**, *61*, 11105.

(9) Tong, X.; Benz, L.; Kemer, P.; Metiu, H.; Bowers, M. T.; Buratto, S. K. *J. Am. Chem. Soc.* **2005**, *127*, 13516.

(10) Basset, J. M.; Lefebvre, F.; Santini, C. *Coord. Chem. Rev.* **1998**, *178*, 1703.

(11) Gunter, P. L. J.; Niemantsverdriet, J. W.; Ribeiro, F. H.; Somorjai, G. A. *Catal. Rev. Sci. Eng.* **1997**, *39*, 77.

(12) Schroeder, T.; Adelt, M.; Richter, B.; Naschitzki, M.; Bäumer, M.; Freund, H.-J. *Surf. Rev. Lett.* **2000**, *7*, 7.

(13) Schroeder, T.; Giorgi, J. B.; Bäumer, M.; Freund, H.-J. *Phys. Rev. B* **2002**, *66*, 165422.

(14) Todorova, T. K.; Sierka, M.; Sauer, J.; Kaya, S.; Weissenrieder, J.; Lu, J.-L.; Gao, H.-J.; Shaikhutdinov, S.; Freund, H.-J. *Phys. Rev. B* **2006**, *73*, 165414.

(15) Ozensoy, E.; Min, B. K.; Santra, A. K.; Goodman, D. W. *J. Phys. Chem. B* **2004**, *108*, 4351.

(16) Kim, Y. D.; Wie, T.; Goodman, D. W. *Langmuir* **2003**, *19*, 354.

(17) Wallace, W. T.; Min, B. K.; Goodman, D. W. *J. Mol. Catal. A: Chem.* **2005**, *228*, 3.

(18) Luo, K.; Kim, Y. D.; Goodman, D. W. *J. Mol. Catal. A: Chem.* **2001**, *167*, 191.

(19) Chen, M. S.; Goodman, D. W. *Surf. Sci.* **2005**, *574*, 259.

(20) Chen, M. S.; Goodman D. W. *Science* **2004**, *306*, 252.

(21) Min, B. K.; Wallace, W. T.; Goodman, D. W. *J. Phys. Chem. B* **2004**, *108*, 14609.

(22) Min, B. K.; Santra, A. K.; Goodman, D. W. *Catal. Today* **2003**, *85*, 113.

(23) Weissenrieder, J.; Kaya, S.; Lu, J. L.; Gao, H. J.; Shaikhutdinov, S.; Freund, H.-J.; Sierka, M.; Todorova, T. K.; Sauer, J. *Phys. Rev. Lett.* **2005**, *95*, 076103.

(24) Ricci, D.; Pacchioni, G. *Phys. Rev. B* **2004**, *69*, 161307.

(25) Todorova, T. K.; Sierka, M.; Sauer, J.; Kaya, S.; Weissenrieder, J.; Lu, J. L.; Gao, H. J.; Shaikhutdinov, S.; Freund, H.-J. *Phys. Rev. B* **2006**, *73*, 165414.

(26) Giordano, L.; Ricci, D.; Pacchioni, G.; Ugliengo, P. *Surf. Sci.* **2005**, *584*, 225.

(27) Sierka, M.; Todorova, T. K.; Kaya, S.; Stacchiola, D.; Weissenrieder, J.; Lu, J.; Gao, H.; Shaikhutdionv, S.; Freund, H.-J.; Sauer, J. *Chem. Phys. Lett.* **2006**, *424*, 115.

(28) Lu, J. L.; Kaya, S.; Weissenrieder, J.; Gao, H.-J.; Shaikhutdinov, S.; Freund, H.-J. *Surf. Sci.* In press.

(29) Giordano, L.; Del Vitto, A.; Pacchioni, G. *J. Chem. Phys.* **2006**, *124*, 034701−7.

(30) Wallace, W. T.; Min, B. K.; Goodman, D. W. *Top. Catal.* **2005**, *34*, 17.

(31) Min, B. K.; Wallace, W. T.; Santra, A. K.; Goodman, D. W. *J. Phys. Chem. B* **2004**, *108*, 16339.

(32) Radzig, V. A. In *Defects in SiO_2 and Related Dielectrics*: *Science and Technology*; Pacchioni, G., Skuja, L., Griscom, D. L., Eds.; NATO Science Series, Series II; Kluwer: Dordrecht, pp 339 and 1999.

(33) Bobyshev, A. A.; Radzig, V. A. *Kinet. Katal.* **1988**, *29*, 638.

(34) Pacchioni, G., Skuja, L., Griscom, D. L., Eds. *Defects in SiO_2 and related dielectrics*: *science and technology*; NATO Science Series II, Kluwer: Dordrecht, 2000.

(35) Beck, J. S.; Vartulli, J. C.; Roth, W. J.; Leonowicz, M. E.; Kregse, C. T.; Schmitt, K. D.; Chu, C. T. W.; Olson, D. H.; Sheppard, E. W.; McCullen, S. B.; Higgins, J. B.; Schlenker, J. L. *J. Am. Chem. Soc.* **1992**, *114*, 10834.

(36) Perdew, J. P.; Chevary, J. A.; Vosko, S. H.; Jackson, K. A.; Pederson, M. R.; Singh, D. J.; Fiolhais, C. *Phys. Rev. B* **1992**, *46*, 6671.

(37) Kresse, G.; Hafner, J. *Phys. Rev. B* **1993**, *47*, 558.

(38) Kresse, G.; Furthmüller, J. *Phys. Rev. B* **1996**, *54*, 11169.

(39) Blöchl, P. E. *Phys. Rev. B* **1994**, *50*, 17953.

(40) Tersoff, J.; Hamann, D. R. *Phys. Rev. B* **1985**, *31*, 805.

(41) Del Vitto, A.; Pacchioni, G.; Lim, K. H.; Rösch, N.; Antonietti, J.-M.; Michalski, M.; Heiz, U.; Jones, H. *J. Phys. Chem. B* **2005**, *109*, 19876.

(42) Antonietti, J.-M.; Michalski, M.; Heiz, U.; Jones, H.; Lim, K. H.; Rösch, N.; Del Vitto, A.; Pacchioni, G. *Phys. Rev. Lett.* **2005**, *94*, 213402.